



# Predicting the Drained Capacity of Skirted Foundations Under Uniaxial Loads

Vali Ghaseminejad<sup>1</sup>(✉), Mohammad Ali Rowshanzamir<sup>2</sup>,  
and Amin Barari<sup>3</sup>

<sup>1</sup> Department of Civil Engineering, Isfahan University of Science and Research,  
Isfahan, Iran

<sup>2</sup> Department of Civil Engineering, Isfahan University of Technology,  
Isfahan, Iran

<sup>3</sup> Department of Civil Engineering, Aalborg University,  
Thomas Manns Vej 23, Aalborg Ø, 9220 Aalborg, Denmark  
abarari@vt.edu

**Abstract.** Skirted foundations denoted as suction caissons are becoming an increasingly prevalent offshore foundation solution for either the oil and gas industry or renewable energy infrastructure. Their response to combined vertical, horizontal and moment loading must be found to ensure their stability under harsh environmental conditions. As part of this process, knowledge of uniaxial capacities is required. Previous studies have neglected effect of deformable ground by assuming that the soil within skirts behaves rigid during drained loading, but this assumption needs rigorous studies. A series of 3-D finite element analyses has been conducted to investigate directly how the skirt geometry, soil strength profile and deformable plug within skirt compartment affect the drained skirted foundation capacity under uniaxial loading. The results show that foundation embedment and soil plug placed within the skirt significantly influence the accompanying mechanisms occurring at failure and therefore the uniaxial capacities.

**Keywords:** Offshore wind turbines · Bucket foundations · Depth factors  
Finite element analyses · Pure bearing capacity · Sand

## 1 Introduction

Offshore wind turbines are sensitive to deformations and tilting [1]. Compared with a monopile, the installation of bucket foundations is easier and does not need heavy installation equipment [2]. Bucket foundations are feasible under suitable soil conditions and are often used in shallow water depths from near-shore to approximately 55 m inland [3]. Wind turbines transfer a small vertical force to the bucket, but develop heavy horizontal loads and moments. Bucket foundations are circular foundations with thin skirts around their circumference consisting of a large steel cylindrical shaft of diameter  $D$ , skirt length  $L$  and skirt thickness  $t_s$ , with a closed top and open bottom. They penetrate into the seabed vertically under self-weight with a trapped soil plug underneath. Penetration discontinues when the lid of the bucket foundation comes in contact with the seafloor.

Gourvenec and Randolph [4, 5], Bransby and Yun [6] and Hung and Kim [7] investigated the responses of two and three-dimensional finite element analyses of the general loading of strip and circular skirted foundations in homogeneous and non-homogeneous clay and presented the ultimate limit states and failure envelopes. Gourvenec [8, 9] surveyed failure envelopes and shape effects on the capacity of shallow foundations under general loading at varying aspect ratios. Gourvenec [10] later studied the effect of embedment on the undrained bearing capacity of shallow strip footings subjected to uniaxial and combined loading through a finite element study. Barari and Ibsen [11–13] reported the experimental and numerical responses of vertical and moment loading on small-scale circular surface and suction bucket models on Baltic clay at Aalborg University. Ibsen et al. [14, 15] investigated the behavior of bucket foundations under combined static loads in dense saturated sand and conducted an extensive experiment on small-scale foundations in the laboratory.

The aim of the current report is to evaluate the effect of aspect ratios and sand relative densities on pure bearing capacities of bucket foundations installed in saturated sands. Load-deformation behavior of suction buckets under pure loads was investigated and compared. Subsequently, the failure mechanism under pure loading based on finite element results was presented.

## 2 Finite Element Model

All FE analyses were performed using Plaxis 3D Foundation software package [16]. For the skirt and the surrounding soil, 15-node wedge elements were used in the 3D finite element calculations. An elastic-plastic model was used to describe the behavior between skirt and soil. Strength reduction factor in the soil-foundation interface was considered  $R_{inter} = 0.7$ . The effect of gaps along the bucket and surrounding soil was prevented. The skirt and lid materials were modeled as linear elastic. External boundaries were set sufficiently remotely to reach sufficient accuracy of the results. Hence the behavior of the bucket foundation is not significantly influenced by the boundary conditions. The length of the finite-element mesh boundary was set to 6 times of the bucket diameter and bottom boundary of the model was extended 3 times the bucket skirt length. In order to determine ultimate horizontal, vertical and moment capacities tangent intersection method is employed. In this methodology, ultimate bearing capacity is obtained as load corresponding to the intersection point of two tangential lines along the initial and latter part of the load-deformation curve. Figure 1 exhibits sign conventions for loads and displacements as well as the finite element mesh.

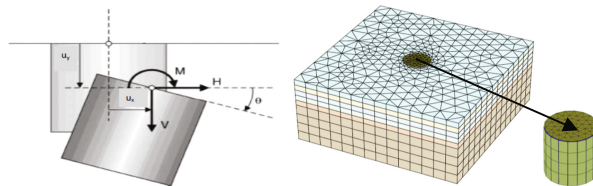


**Fig. 1.** Left: Sign convention for loads and displacements, Right: A Schematic view of the finite element mesh used in the analyses

Bucket foundations embedded in sands with different relative densities at  $D = 12$  m, 16 m and different aspect ratios ( $L/D = 0, 0.25, 0.5, 0.75, 1$ ) were used.  $D$  refers to the diameter of the bucket foundation and  $L$  is skirt length of the bucket. In the analysis, deformation properties of steel materials with modulus of elasticity  $E = 210$  GPa and Poisson's ratio  $\nu = 0.2$  were considered. Submerged unit weight of the steel used for the bucket body was set to  $\gamma' = 68$  kN/m<sup>3</sup>. A top plate thickness of  $t_L = 0.10$  m and unit weight  $\gamma' = 77$  kN/m<sup>3</sup> and a very large modulus of elasticity  $E = 1 \times 10^9$  GPa were selected for the bucket lid. The analyses are divided into three stages. The initial step is used to consider soil normal stresses by applying unit weight of soil. In the second phase, a part of the soil is replaced by the steel bucket elements. Center top of the bucket foundation is loaded gradually during the third phase until failure. Pure horizontal, vertical and moment loads were applied separately on the bucket lid and increased gradually until the pure bearing capacity of the bucket foundation was reached. In this research, Mohr–Coulomb material model is used as constitutive model in the numerical simulation of soil behavior. To simulate non-linear soil response, stress-dependency of the oedometric modulus of elasticity was implemented through the following expression.

$$E_S = \kappa \cdot \sigma_{at} \cdot \left( \frac{\sigma_m}{\sigma_{at}} \right)^\lambda \quad (1)$$

Where  $\sigma_m$  is the current mean principle stress in the considered soil element and  $\sigma_{at} = 100$  kN/m<sup>2</sup> is reference stress. Parameters  $\kappa$  and  $\lambda$  are related to soil stiffness at reference stress state. Table 1 gives the parameters of the material used for sands with different properties.

**Table 1.** Material properties used in the numerical analysis [17]

Property	Loose sand	Medium dense sand	Dense sand	Unit
Submerged unit weight ( $\gamma'$ )	7	9	11	[kN/m <sup>3</sup> ]
Oedometric stiffness parameter ( $\kappa$ )	300	400	600	[-]
Oedometric stiffness parameter ( $\lambda$ )	0.65	0.6	0.55	[-]
Poisson's ratio ( $\nu$ )	0.25	0.25	0.25	[-]
Internal friction angle ( $\phi'$ )	30	35	40	[°]
Dilation angle ( $\psi$ )	2.5	5	10	[°]
Cohesion ( $C'$ )	0.1	0.1	0.1	[kN/m <sup>2</sup> ]

### 3 Validation of the Numerical Model

In this study, a finite element simulation of bucket foundations in dense sand was utilized and validated versus the results of finite element analysis performed by Achmus et al. [17]. A bucket at  $D = 12$  m, a skirt length of  $L = 9$  m ( $L/D = 0.75$ ) and a skirt thickness of  $t_s = 3$  cm was analyzed. Dense soil parameters listed in Table 1, were chosen for analysis. Figure 2 compares Achmus et al. results along with the numerical simulations and loading eccentricity of  $h = 100$  m. Moment-rotation curve represented good agreement with the literature.

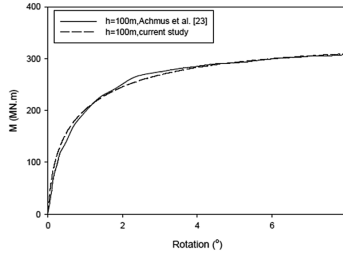


Fig. 2. Moment-rotation curve for the FE simulation compared by Achmus et al. [17] results

### 4 Vertical Capacity

Vertical loads on bucket foundations derive from their self-weight as well as the loading tower. Figure 3 shows view of vertical displacement contours under pure vertical loading at  $D = 16$  m for  $L/D = 0.25$  and 1. Failure under pure vertical loads was almost governed by pure vertical displacements. Figure 4 shows variations in pure vertical capacity depth factors ( $d_{cv} = V_{ult(L/D)} / V_{ult(L/D=0)}$ ) as a function of aspect ratios for a range of sand profiles using  $D = 12$  m and 16 m. At large aspect ratios, bucket foundations in different sands represented higher vertical bearing capacities since their sidewalls involved higher shear strengths.

There is no exact solution to determine the pure vertical capacity of a bucket foundation. However, the results of the present study showed that a linear function could be considered in  $V/V_{ult} - L/D$  curve at different diameters and sand types.

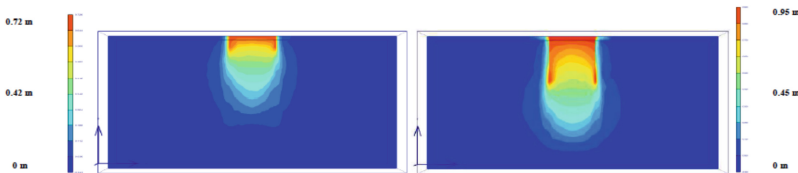


Fig. 3. Vertical displacement contours under pure vertical loading in medium dense sand at  $D = 16$  m, Left:  $L/D = 0.25$  Right:  $L/D = 1$

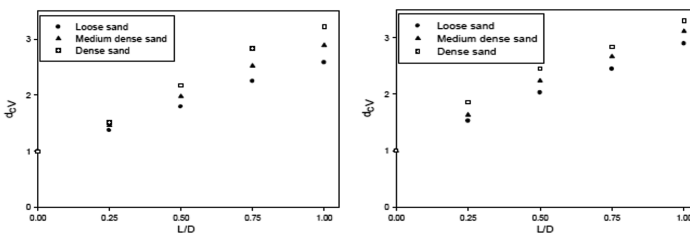


Fig. 4. Normalized pure vertical bearing capacities as a function of aspect ratios in sands with different relative densities, Left:  $D = 12$  m, Right:  $D = 16$  m

Additionally, to determine pure vertical bearing capacity depth factors, the following equations were found to better match with the numerical results.

$$d_{cV} = 1 + 1.77 \left( \frac{L}{D} \right) \quad \text{loose sand} \quad (2)$$

$$d_{cV} = 1 + 2.07 \left( \frac{L}{D} \right) \quad \text{medium sand} \quad (3)$$

$$d_{cV} = 1 + 2.41 \left( \frac{L}{D} \right) \quad \text{dense sand} \quad (4)$$

It is worth adding that the results could be valid for large diameter buckets when  $0 \leq L/D \leq 1$ . At diameter of 16 m, the pure vertical capacity depth factor was a little larger than 12 m. However, in order to reach a unique response regarding both 12 m and 16 m in sands with different relative densities, the same equation was considered.

## 5 Horizontal Capacity

Since the analysis of horizontal bearing capacities could have a great role in offshore wind turbines, an investigation of the behavior of bucket foundations with varying soil profiles to pure horizontal load was performed. Figure 5 shows view of incremental displacement contours under pure horizontal loading at  $D = 16$  m for  $L/D = 0.25$  and 1. Sliding failure mechanism of surface foundations in pure horizontal loads alters from sliding behavior to a rotational mode when skirts are applied to different types of sand under investigation here. In pure horizontal loading, the coupling between the horizontal and rotational degrees of freedom played an important role. The rotational mechanism observed in terms of pure horizontal loading, was related to lateral strength of soil acting on inside and outside the bucket skirt.

Figure 6 illustrates variations in pure horizontal capacity depth factors ( $d_{cH} = H_{ult(L/D)} / H_{ult(L/D=0)}$ ) as a function of aspect ratios in loose, medium and dense sands at  $D = 12$  m, and 16 m. Finite element results indicated that pure horizontal capacity depth factors could be related to the linear expressions between normalized ultimate uniaxial horizontal loads and aspect ratios.

$$d_{cH} = 1 + 8.36 \left( \frac{L}{D} \right) \quad \text{loose sand} \quad (5)$$

$$d_{cH} = 1 + 9.53 \left( \frac{L}{D} \right) \quad \text{medium sand} \quad (6)$$

$$d_{cH} = 1 + 10.34 \left( \frac{L}{D} \right) \quad \text{dense sand} \quad (7)$$

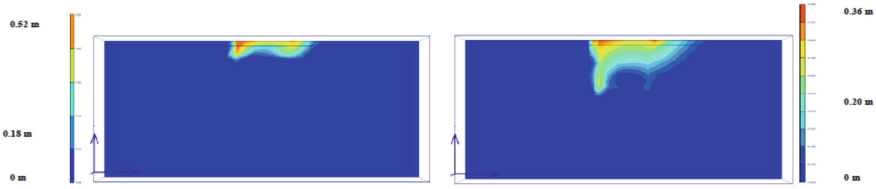


Fig. 5. Incremental displacement contours under pure horizontal loading in medium dense sand at  $D = 16$  m, Left:  $L/D = 0.25$  Right:  $L/D = 1$

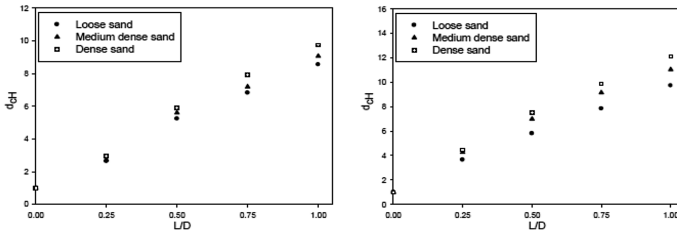


Fig. 6. Normalized pure horizontal capacities as a function of aspect ratios in sands with different relative densities, Left:  $D = 12$  m, Right:  $D = 16$  m

## 6 Moment Capacity

Moment loading is worth consideration in wind turbines, which are tall and slender structures and as a result susceptible to overturn due to eccentricity of loading. The wind at the top of the tower can produce huge moments for the bucket foundation to bear compared to vertical and horizontal loading imposed on it. Figure 7 outlines incremental displacement contours under pure moment loading at  $D = 16$  m for  $L/D = 0.25$  and 1. At large aspect ratios, the soil confined within the bucket foundation was observed to behave as a rigid cluster during loading, whereas in case of low aspect ratios it was affected by the failure mode. A pure rotation would not accompany large deformations under pure moment due to a combination of horizontal and rotational degrees of freedom causing horizontal and rotational translations.

Figure 8 illustrates variations in pure moment capacity depth factors ( $d_{cM} = M_{ult(L/D)}/M_{ult(L/D=0)}$ ) as a function of aspect ratios in all types of the sands at  $D = 12$  m and 16 m. At small aspect ratios, the pure moment bearing capacity was small, meaning that sidewalls could be negligible, and increases in the strength of underlying soil would induce more capacity to bucket foundations. The pure moment capacity was larger in dense sand than medium and loose sands. When the degree of embedment increases, the difference will become greater.

Finite element results indicated that pure moment capacity depth factors could be related to the square of aspect ratios and expressed by the following functions.

$$d_{cM} = 1 + 2.22 \left(\frac{L}{D}\right) + 7.22 \left(\frac{L}{D}\right)^2 \quad \text{loose sand} \quad (8)$$

$$d_{cM} = 1 + 1.73 \left(\frac{L}{D}\right) + 8.94 \left(\frac{L}{D}\right)^2 \quad \text{medium sand} \quad (9)$$

$$d_{cM} = 1 + 2.12 \left(\frac{L}{D}\right) + 10.95 \left(\frac{L}{D}\right)^2 \quad \text{dense sand} \quad (10)$$

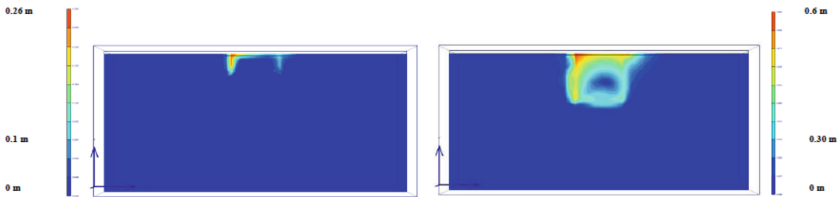


Fig. 7. Incremental displacement contours under pure moment loading in medium dense sand at  $D = 16$  m, Left:  $L/D = 0.25$ , Right:  $L/D = 1$

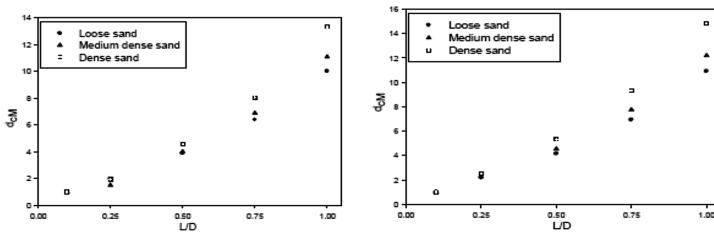


Fig. 8. Normalized pure moment capacities as a function of aspect ratios in sands with different relative densities, Left:  $D = 12$  m, Right:  $D = 16$  m

## 7 Conclusion

The study investigated the results of three-dimensional numerical analyses of bucket foundations founded in loose, medium and dense sands under pure horizontal, vertical and moment loadings. The influence of variations in the geometry of the bucket (length-to-diameter aspect ratio  $L/D$ ) and soil properties on pure bearing capacity were evaluated and discussed. Bucket dimensions and types of sand would significantly affect pure ultimate capacities of bucket foundations. Sidewalls in bucket foundations proved to play an important role in soil-bucket foundation response to uniaxial loadings, being able to transfer the normal and shear stresses to the soil. The effect of embedment was examined and depth factor relationships were developed for a range of soil properties. The normalized expressions of pure horizontal and vertical bearing capacities were found to be proportional to aspect ratios linearly, while a quadratic relationship was observed between aspect ratio and pure moment capacity depth factor. As depicted above, failure under pure horizontal and moment loads may be governed by a combination of horizontal and rotational translations.

## References

1. Barari, A., Bagheri, M., Rouainia, M., Ibsen, L.B.: Deformation mechanisms for Monopile foundations of offshore wind power plants considering the cyclic mobility effect. *Soil Dyn. Earthq. Eng.* **97**, 439–453 (2017a)
2. Barari, A.: Characteristic behavior of bucket foundations. Aalborg University, Denmark, Ph. D. thesis (2012)
3. Barari, A., Ibsen, L.B., Taghavi Ghalesari, A., Larsen, K.A.: Embedment effects on vertical bearing capacity of offshore Bucket foundations on cohesionless soil. *Int. J. Geomech.* (2017b). [https://doi.org/10.1061/\(ASCE\)GM.1943-5622.0000782](https://doi.org/10.1061/(ASCE)GM.1943-5622.0000782)
4. Gourvenec, S., Randolph, M.: Effect of strength non-homogeneity on the bearing capacity of circular skirted foundations subjected to combined loading. In: Proceedings of the Twelfth International Offshore and Polar Engineering Conference, Kitakyushu, Japan (2002)
5. Gourvenec, S., Randolph, M.: Bearing capacity of a skirted foundation under VMH loading. In: Proceedings of OMAE03 22nd International Conference on Offshore Mechanics and Arctic Engineering, Cancun, Mexico (2003)
6. Bransby, M.F., Yun, G.J.: The undrained capacity of skirted strip foundations under combined loading. *Géotechnique* **59**(2), 115–125 (2009)
7. Hung, L.C., Kim, S.R.: Evaluation of vertical and horizontal bearing capacities of bucket foundations in clay. *Ocean Eng.* **52**, 75–82 (2012)
8. Gourvenec, S.: Shape effects on the capacity of rectangular footings under general loading. *Géotechnique* **57**(8), 637–646 (2007)
9. Gourvenec, S.: Failure envelopes for offshore shallow foundations under general loading. *Géotechnique* **57**(9), 715–728 (2007)
10. Gourvenec, S.: Effect of embedment on the undrained capacity of shallow foundations under general loading. *Géotechnique* **58**(3), 177–185 (2008)
11. Barari, A., Ibsen, L.B.: Effect of embedment on the vertical bearing capacity of Bucket foundations in clay. In: Proceedings, Pan-Am CGS Geotechnical Conference, Toronto, Ont (2011)
12. Barari, A., Ibsen, L.B.: Undrained response of bucket foundations to moment loading. *Appl. Ocean Res.* **36**, 12–21 (2012). <https://doi.org/10.1016/j.apor.2012.01.003>
13. Barari, A., Ibsen, L.B.: Vertical capacity of bucket foundations in undrained soil. *J. Civ. Eng. Manag.* **20**(3), 360–371 (2014)
14. Ibsen, L.B., Barari, A., Larsen, A.: Adaptive plasticity model for bucket foundations. *J. Eng. Mech.* **140**, 361–373 (2014)
15. Ibsen, L.B., Larsen, K.A., Barari, A.: Calibration of failure criteria for bucket foundations on drained sand under general loading. *J. Geotech. Geoenviron. Eng.* (2014). [https://doi.org/10.1061/\(ASCE\)GT.1943-5606.0000995](https://doi.org/10.1061/(ASCE)GT.1943-5606.0000995)
16. Plaxis user's manual, version 1.6 (2005)
17. Achmus, M., Akdag, C.T., Thielen, K.: Load-bearing behavior of suction bucket foundations in sand. *Appl. Ocean Res.* **43**, 157–165 (2013)